



The Applications of New Inorganic Polymer for Adsorption Cadmium from Waste Water

Nataša Mladenović¹ · Ljiljana Kljajević^{2,4} · Snežana Nenadović^{2,4} · Marija Ivanović² · Bojan Čalija³ · Jelena Gulicovski^{2,4} · Katarina Trivunac¹

Received: 11 March 2019 / Accepted: 31 May 2019 / Published online: 8 June 2019
© Springer Science+Business Media, LLC, part of Springer Nature 2019

Abstract

Fundamental research of inorganic polymers prepared from available aluminosilicate precursors represent an innovative class of materials characterized by low energy consumption for production. This is just one of the reasons why their use is focused in protecting the environment for removing of heavy metals from aqueous solutions. The concentration of hydroxide as activator solution plays an important role in the geopolymerization process. The present study examined the use of geopolymer materials, obtained in reaction of geopolymerizations of metakaolin as precursor activated with NaOH concentration 2.0, 4.0, 6.0 and 8.0 mol/dm³ for removal of cadmium ions from aqueous solutions. The structure and properties of the obtained geopolymer samples were studied by X-ray diffraction (XRD), scanning electron microscopy (SEM) and diffuse reflection infrared spectroscopy (DRIFTS). To investigate the surface charge of geopolymers the zeta potential measurements were performed. Batch adsorption experiments conducted at room temperature (23 ± 1 °C) showed that the adsorption pattern followed the Freundlich isotherm model. The maximum removal of cadmium obtained from batch studies was 84.1% for GP6M at pH ≈ 6.7. The results generally showed that geopolymer samples could be considered as a potential adsorbent for cadmium removal from aqueous solutions.

Keywords Geopolymer · DRIFT · Chemical properties · Functional applications · Freundlich isotherm model

1 Introduction

Heavy metals, lead (Pb), chromium (Cr), copper (Cu), cadmium (Cd), nickel (Ni), and zinc (Zn) are source of same concern because of their possible reactivity, toxicity and mobility in the water and soil. They are classified as human carcinogens according to the International Agency for Research on Cancer. Cadmium is a heavy metal of

considerable environmental and occupational concern. The highest level of cadmium compounds in the environment is accumulated in the sedimentary rocks, but it is frequently used in various industrial activities, such as pigments, batteries, fertilizers and pesticides [1, 2]. Cadmium is released into natural waters by industrial and domestic wastewater discharges. In humans, it's accumulated in the kidneys which will begin to malfunction at overdoses spilling proteins in the urine and disrupting protein metabolism. It is well known that chronic cadmium toxicity has been the cause of Japanese Itai–Itai disease [3].

Adsorption is a very promising method for reducing cadmium concentrations in potable waters, because it is a relatively simple, efficient and low-cost technique. There are different adsorbents which were used for the adsorption of heavy metals from waste water. Commonly used adsorbent for the removal of pollutants present in water and wastewaters is activated carbon. Its price is high, so the synthesis of new equally effective adsorbents is very desirable [4, 5]. Geopolymers are usually obtained through inexpensive and ecofriendly synthetic procedures with low waste gas

✉ Ljiljana Kljajević
ljiljana@vin.bg.ac.rs

¹ Faculty of Technology and Metallurgy, University of Belgrade, Belgrade, Serbia

² Laboratory for Materials Sciences, Vinča Institute of Nuclear Sciences, University of Belgrade, Belgrade, Serbia

³ Department of Pharmaceutical Technology and Cosmetology, University of Belgrade, Belgrade, Serbia

⁴ Center for the Synthesis, Processing and Characterization of Materials for Use in Extreme Conditions “CEXTREME LAB”, Vinča Institute of Nuclear Sciences, University of Belgrade, Belgrade, Serbia

emission [6–9]. That is the one of the reason why they are called the “green materials”. Geopolymers synthesized at temperatures below 90 °C by alkali activation of highly reactive metakaolin as a good source of silicon and aluminium [10]. Geopolymerization mechanism involves dissolving aluminum and silicon in alkaline solution, transport and orientation of dissolved species accompanied by polycondensation and the creation of three-dimensional aluminosilicate networks. Beside the temperature another important parameter is the duration. The samples at an elevated temperature were usually retained 12 or 24 h [11]. The concentration of hydroxide in the solution of activator plays an important role in the process of geopolymerization. Studies of the effect of hydroxide led to important discoveries about the mechanism of the reaction. If working with highly concentrated hydroxide solution (10 mol/dm³ and more), the pH will be sufficiently high to reach the dissolution of silicon from the raw material as well as to prevent the dissolution of the Ca (OH)₂ [12]. The charging of particles in aqueous solutions is a factor that is significant for ion adsorption. Zeta potential is the most prominent parameter used to describe the surface–force interaction and the stability of particles in suspension. Since pH-dependent surface charging is a very important subject of research to define the state of the surface of a dispersed solid phase, measurements of zeta potential are major.

The researchers have mainly dealt with the influence of NaOH concentration on the compressive strength and mechanical properties of geopolymers [13–19]. The objectives of this study were to investigate effectiveness of synthesized geopolymer samples, activated by different NaOH concentration, for removal of cadmium from aqueous solutions.

2 Materials and Methods

For the synthesis of geopolymer samples thermally treated kaolinite (Rudovci, Lazarevac, Serbia) at 750 °C for 1 h was used. The structural characteristics of kaolinite were investigated in researching by Nenadović et al. [20]. The alkaline activator solutions were prepared from sodium silicate (volume ratio Na₂SiO₃/NaOH = 1.6) and 2 M, 4 M, 6 M and 8 M NaOH solutions (analytical grade). The geopolymer samples (GP) were synthesized from metakaolin (MK) and the alkaline activator solution (solid/liquid ratio was approximately one), which were mixed for 15 min and then left at room temperature for 24 h. Finally, the mixture was kept in a sample drying oven for 48 h at 60 °C. Prepared geopolymer samples were labeled as GP2M, GP4M, GP6M and GP8M. After that, the dry samples were milled and sifted through a sieve with hole diameter of 355 μm. Prior to the adsorption, the samples were stored in a desiccator in the covered containers.

All samples were characterized by X-ray diffractometry (XRD) by using Ultima IV Rigaku diffractometer, equipped by Cu Kα_{1,2} radiation, with a generator voltage of 40.0 kV and a generator current of 40.0 mA. The 2θ range of 5–80° was used for all powders in a continuous scan mode with a scanning step size of 0.02° at scan rate of 5°/min. The functional groups of all obtained samples were studied using DRIFT spectroscopy. Spectral information of diffuse reflection FT-IR spectra was analysed and compared. DRIFT spectra were obtained using Spectrum Two spectrometer and were recorded at 4 cm⁻¹ resolution. Approximately 5% of samples were dispersed in oven-dried spectroscopic grade potassium bromide (KBr) with refractive index of 1.559 and the particle size of 5–20 μm. Spectra was taken at room temperature. Background KBr spectra obtained and spectra rationed to the background. The spectral data of the samples were collected in the 4000–400 cm⁻¹ region.

The microstructure analysis of obtained geopolymer samples was performed on Au-coated samples using JEOL JSM 6390 LV electron microscope at 25 kV coupled with EDS (Oxford Instruments X-Max^N). To investigate the influence of pH value on colloidal stability and determine isoelectrical point (IEP) of investigated geopolymer samples, zeta potential measurements were performed in pH range between 2 and 12. Investigated samples were dispersed in ultra-pure water (Milli-Q purification system, Millipore, USA) on a magnetic stirrer to obtain 0.1 g/l dispersions. The pH value of the resulting dispersions was measured using a HI 2223 pH meter (Hanna Instruments, SAD) and adjusted by adding 0.1 M NaOH and HCl solutions. To ensure complete redispersion prior zeta potential measurements, the colloidal dispersions were sonicated in a Sonorex RK 102 H ultrasonic bath (Bandelin, Germany) and transferred to disposable folded capillary DTS1070. Zeta potential was determined by Laser Doppler Electrophoresis using a Zetasizer NanoZS instrument (Malvern Instruments Ltd., UK). All the measurements were performed in a triplicate at 25 °C. The average values of zeta potential were calculated and expressed as a function of pH.

Adsorption tests at room temperature to investigate the influences of different parameters on the effectiveness geopolymer samples on cadmium adsorption were performed. Solution of Cd (II) ion was prepared by dissolving CdCl₂·2 ½ H₂O in deionized water. The pH of the solutions was adjusted with few drops of HCl to a desired value. After adsorption, the solution was filtered and the filtrate was analyzed for cadmium concentration by flame atomic absorption spectrophotometry (FAAS Pye Unicam) at 228.8 nm. The experimental parameters such as contact time, initial concentrations, mass of adsorbent, pH of the sample solutions were tested to study their effects on the removal of Cd (II) by the geopolymer samples. The removal efficiency, R, of geopolymer samples were calculated with Eq. (1):

$$R = \frac{(c_0 - c_e)}{c_0} \times 100 \quad (1)$$

where the c_0 and c_e (mg/l) are the initial and the final concentration of Cd(II) in the solution, respectively.

The adsorption capacity, q_e (mg/g), was calculated with Eq. (2):

$$q_e = \frac{(c_0 - c_e)V}{m} \quad (2)$$

where V represents volume of the solution and m is the mass of the adsorbent.

3 Results and Discussion

The structural changes that occur during the geopolymerization of the alkali activated materials have been followed as a function of the sodium hydroxide (NaOH) concentration (2–8 M) and time by FT-IR and XRD analysis. The curing and in the same time aging of geopolymer samples has been followed for 28 days.

3.1 Structural Characterization of MK and GP Samples

Figure 1 shows the XRD patterns of the geopolymers cured 28 days. The geopolymers are obtained by reaction of metakaolin and alkali activator solutions. Four samples of geopolymers were analyzed (GP2M, GP4M, GP6M and GP8M).

XRD analysis of all geopolymer samples revealed their amorphous-like structure with the position of an amorphous halo in the range 18–32°. This amorphous halo indicates

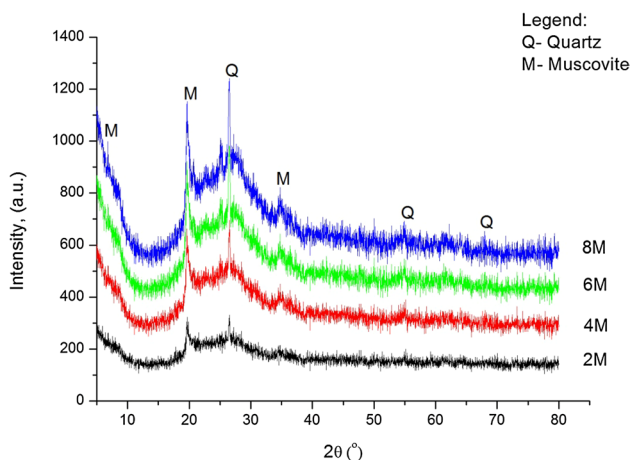


Fig. 1 X-ray diffractogram of **a** geopolymer GP2M **b** geopolymer GP4M **c** geopolymer GP6M **d** geopolymer GP8M after 28th days of aging

short range ordering of the samples. SiO_2 (α -quartz) (ICSD 156198) and Muscovite (ICSD 17049) as a crystalline phases are appeared. The intensity of the peaks depends on the crystallization of the phases, which may be attributed to age of cured or alkalinity of obtained paste causing variables on the geopolymers. The intensity of the XRD peaks of quartz as well as muscovite does not change significantly. This is a normal behavior of quartz at low temperatures and in medium alkaline solutions is not expected it's dissolving. Furthermore, several authors [12, 21–23] have noted the dissolution of the aluminosilicates from the raw materials and the recrystallization of new semi-crystalline phases appeared at later stages of curing. Considering that a rather large noise of the XRD-s is obtained, it is possible that has come to a lesser extent until the formation of some crystalline phases (Zeolit X, pdf 00-026-0898), for which it is not possible to claim certainty their presence. The main difference with the current work is that the appearance of new phases has not been noticed, perhaps because enhance of alkalinity of liquid phase do not effect on the formation new crystalline phase.

DRIFT is a surface localized FTIR spectroscopy, since it can provide both chemical and structural information for all types of solid surfaces [24].

The diffuse reflection infrared Fourier transform spectroscopy (DRIFTS) technique is extremely useful for non-transparent materials and/or for in situ measurements at elevated temperature [25].

Since the optical phenomena that generate DRIFT signals are different from those involved in transmittance spectrometry, the spectra obtained by these methods cannot be considered equivalent according to researching of Italian scientists [26]. The DRIFT spectrum of the geopolymers (Fig. 4a, c, d) shows broad bands at about 3700–3450 cm^{-1} and relatively broad band at 1620 cm^{-1} due to O–H stretching and bending modes of absorbed molecular water [27, 28]. The difference of GP4 M as compared to other geopolymer samples (Fig. 4b) is in the occurrence the two peaks near 3700 cm^{-1} and 3610 cm^{-1} . The appearance the sharp peaks near 3700 cm^{-1} and 3610 cm^{-1} could be the consequence of the remains of kaolinite. Kaolinite was not detected by XRD, due to quite a large noise of the spectrum (Fig. 1). The considerably reduced absorption band at 2880 cm^{-1} , pronounced in all geopolymer samples, indicate presence of organic matter (aliphatic structures) [29]. The appearance of band at about 1045 cm^{-1} was due to Si–O stretching vibrations [28]. Shifting the band to the right side, toward the lower wave number, indicates the condensation of Si–O tetrahedra in geopolymer [28, 30]. The Si–O bending band (905 cm^{-1}) is found in the range 890–975 cm^{-1} [31–34]. It is important to point out that the characteristic metakaolin Si–O–Al band at 810 cm^{-1} due to the six-coordinated Al(VI)–O stretching vibration, disappears in the geopolymer indicating a geopolymerization reaction [28]. According to

the literature, there are vibration bands attributed to Secondary Building Units (SBUs) in the 800–550 cm^{-1} region. SBUs are made of joined SiO_4 and AlO_4 tetrahedrals, forming variously membered rings [31]. In our case, in this range, vibrational bands appear at 691 and 541 cm^{-1} . The vibrational bands at 905, 691 and 541 cm^{-1} are almost not visible in GP8 M (Fig. 2d). The peak between 800 and 700 cm^{-1} is due to Al–O vibrations coming from isolated tetrahedral or pentahedral aluminum [35]. Finally, the signal at about 466 cm^{-1} is due to Si–O bending vibration [28, 36, 37].

This study focused on analyzing the microstructure of the geopolymer formed after 28 days of curing. The different types of morphologies formed during the geopolymerisation process. Subsequently, NaOH alkaline activator drains out metakaolin particle resulting in polymeric gel formation [24]. The microstructure of metakaolin powder is presented at SEM micrographs of Fig. 3.

The surfaces of the powdered materials cured at 60 °C for 2 days and aging 28 days are shown in Fig. 4a–d respectively. After 28 day of aging, the overall semi crystal morphology of the geopolymer samples had evolved. These crystallites were about 0.5 μm of thick. The microstructures of the samples obtained using different concentration of NaOH are similar. The samples show a porous microstructure formed by unreacted micron size particles and a geopolymeric matrix that is formed during the polycondensation. The microstructures of GP2M, GP4M and GP6M (Fig. 4a–c)

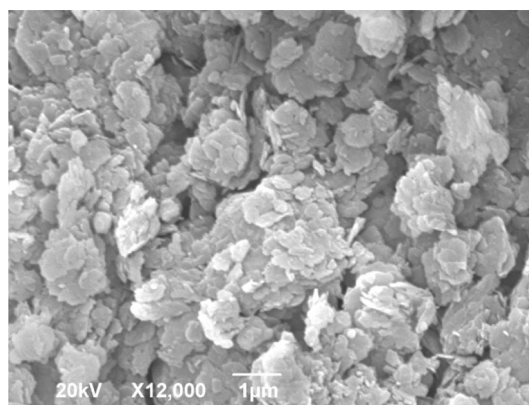


Fig. 3 SEM micrographs of MK

show intergranular cracks that indicate the interfaces are weak. All geopolymer samples after 28 days of aging show the microstructure consists of dense plates formed by the geopolymerization with a group of crystalline sticks that in some places merge that are attributed to the recrystallization of the some kind of silica. However, the geopolymer dense plates that are observed indicate that these are the strongest constituents.

Table 1 shows elements that are identified in MK and geopolymer samples. As we can see the percent of some of the elements decrease with increasing concentration of

Fig. 2 DRIFT spectra of geopolymer samples a GP2M; b GP4M; c GP6M; d GP8M

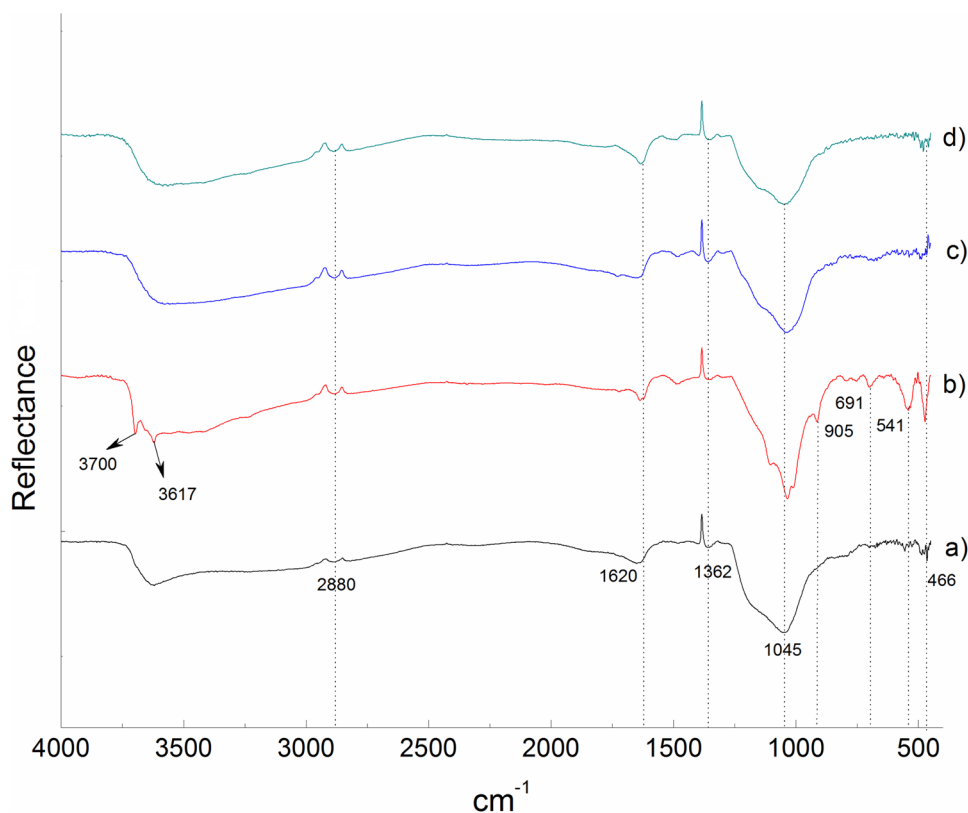


Fig. 4 SEM micrographs of GP samples, **a** GP2M, **b** GP4M, **c** GP6M and **d** GP8M

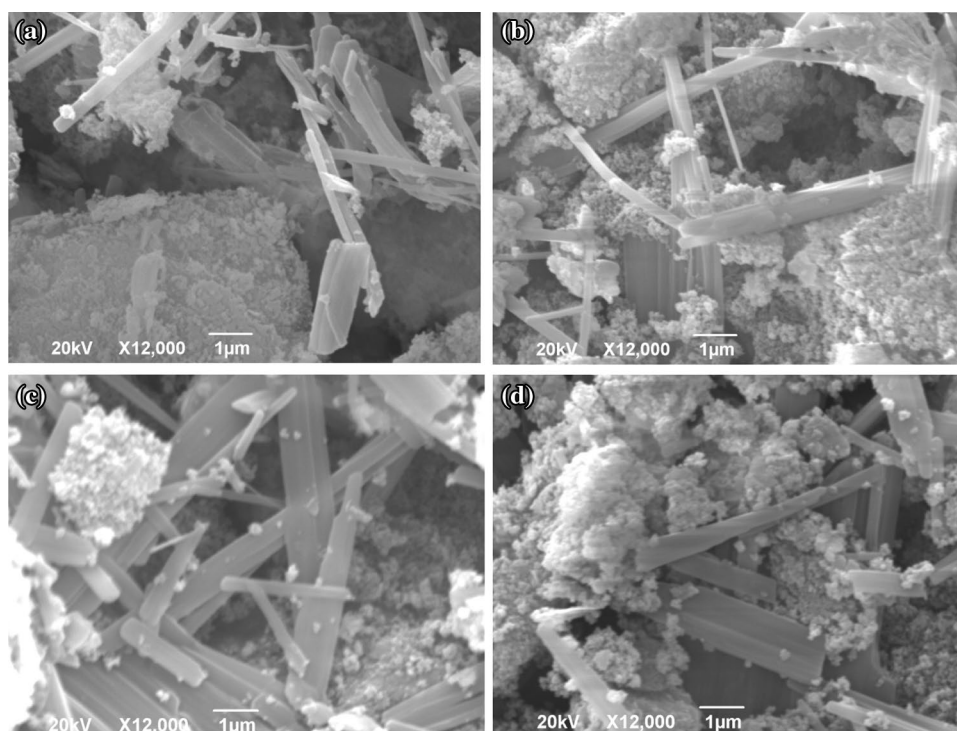


Table 1 The elemental analysis of metakaolin and geopolymer samples

Element	MK Wt%	GP2M Wt%	GP4M Wt%	GP6M Wt%	GP8M Wt%
O	44.42	49.02	48.78	53.95	54.29
Na	–	5.70	7.45	12.61	11.78
Mg	0.35	–	0.24	–	–
Al	19.84	13.73	11.41	8.91	8.85
Si	23.39	21.69	21.56	16.86	16.87
K	0.79	0.59	0.41	0.32	0.29
Ca	0.42	0.32	0.24	0.17	0.17
Fe	2.04	1.55	1.04	0.86	0.74
Cu	2.77	2.59	2.79	1.07	1.72
Zn	2.23	1.72	2.24	0.84	1.40
Si/Al	1.18	1.58	1.89	1.89	1.91

NaOH, such as Al and Si. The percentage of these elements is reduced to the account of the increase in Na and oxygen contents introduced into the system via NaOH and Na_2SiO_3 . Wt% Na in GP8 M is somewhat lower than wt% Na in GP6M. The inhomogeneity of the samples must be taken into account, which therefore influences the composition of the examined surface of the sample. EDS analysis show that with an increase in molarity of NaOH over 4 M the Si/Al ratio isn't increasing. Since it is a surface analysis, the conclusion can't be general or applicable to the whole sample.

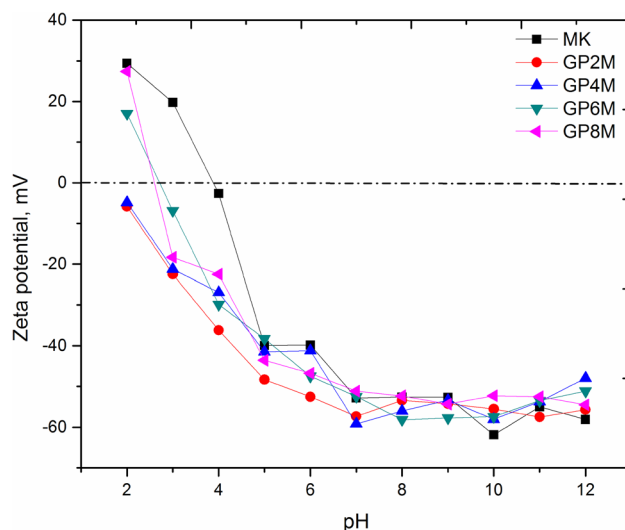


Fig. 5 Zeta potential of **a** MK, **b** GP2M, **c** GP4M, **d** GP6M and **e** GP8M

3.2 Surface Charge of Geopolymers

Figure 5 show the function of zeta potential from pH in the geopolymer samples and as well as metakaolin–water system. The MK with negative zeta potentials (Fig. 5a) will react more readily, due to the excess of reactive silicate and aluminate groups on the surface. The zeta potentials of the all geopolymers gave negative values, Fig. 5. Also, the high concentration of alumina and silica functional groups is

present at the surface of the geopolymer which is confirmed by DRIFT analysis.

According to the literature, we assumed metakaolin react with NaOH/Na₂SiO₃ aqueous solution, the aluminate and the silicate species hence a negatively charged surface is formed while establishing a double layer. The Na⁺ ions of the alkaline activator, will react with aluminate and silicate negatively charged surface groups and form a sodium aluminosilicate gel layer. Decreasing of zeta potential of geopolymer gel is due to the accumulation of more Na⁺ ions in a double layer [38]. In our case all geopolymer samples in range of pH from 2.0 to 8.0 have the smallest zeta potential in relation with metakaolin sample. The GP6M geopolymer has the smallest value of zeta potential at pH 8.0. The small zeta potential would indicate that the GP6M geopolymer will more readily form the gel layer. It is characteristic the lowest values of zeta potential for all samples occur at pH around 7. After increasing the pH, there is no significant change in the zeta potential.

3.3 Adsorption of Cadmium Ions

Different experimental parameters, such as pH, mass of adsorbents, initial concentrations of the sample solution and contact time were tested to study their effects on the removal of cadmium, in bath process on the room temperature, onto prepared geopolymers.

3.3.1 Effect of Contact Time and pH on Adsorption of Cd(II) Ions

The dependence of the adsorption capacity on time was tested in the range of 5–120 min. Figure 6 shows that the process took place quickly, after 15 min it came to 80% of the equilibrium capacity. After 60 min, a plateau was reached, so this value was selected for investigation of the influence of other parameters. The highest value of adsorption capacity had been achieved when the GP6M geopolymer was used for adsorption.

The negatively charged geopolymer surface area will facilitate adsorption of positively charged ions such as heavy metal ions. The binding of metal ions to active sites on the adsorbent is carried out mainly by ion exchange or complexation. Since the pH value affects both the surface charge of adsorbent and the ionic forms of the metal, it can be said that it has significant influence onto adsorption process.

As shown in previous section the increase of pH values above 7 does not lead to a significant change of the value of zeta potential, due to influence of pH on the adsorption capacity of the geopolymer adsorbents for Cd(II) ions was examined in the range 2.0–7.0, Fig. 7.

In highly acidic solutions a significant amount of H⁺ ions was present. The competition between ions for available sites

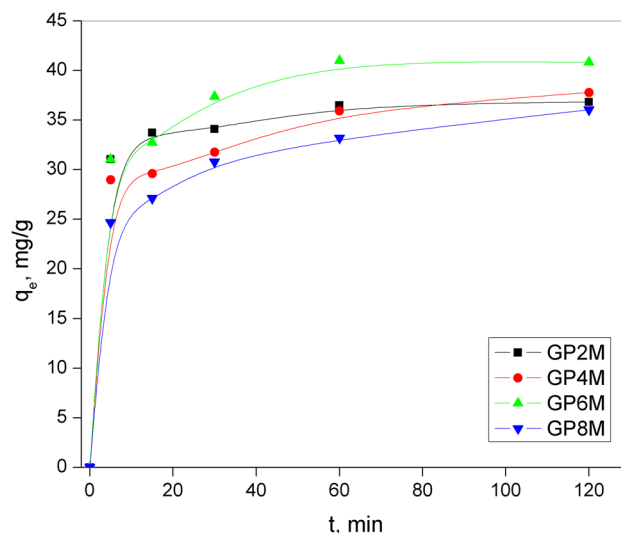


Fig. 6 Influence of contact time on adsorption capacity of geopolymer samples ($c_0 = 50 \text{ mg/dm}^3$, $m_{GP} = 0.2500 \text{ g}$, $\text{pH} = 6.7$)

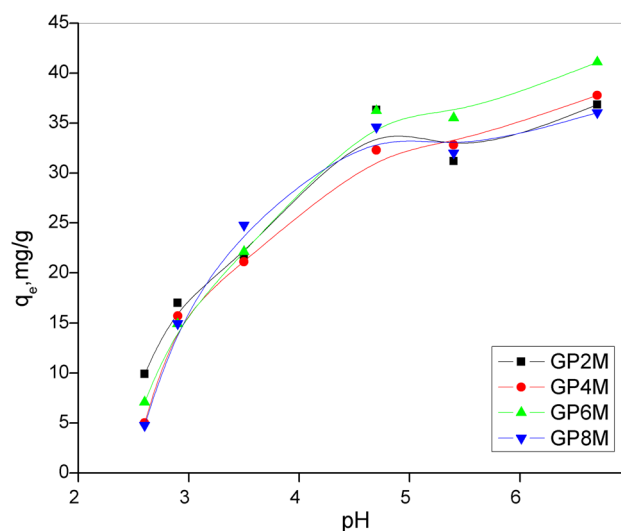


Fig. 7 Influence of pH on adsorption capacity of geopolymer samples ($c_0 = 50 \text{ mg/dm}^3$, $t = 60 \text{ min}$, $m_{GP} = 0.2500 \text{ g}$)

on the geopolymer surface occurred, so adsorption of Cd(II) ions was low. By increasing the pH above 5.0, Cd(II) ions became dominant in the solution and the adsorption capacity increased. A plot of the ionic form of cadmium and the pH of the solution indicates that up to pH 8, cadmium is in the form of Cd²⁺, while further increase of the pH leads to the formation of ion Cd(OH)⁺, and at the end to the formation of Cd(OH)₂ [39]. Also, according to zeta potential measurement, the GP6M geopolymer has the smallest value of zeta potential at pH 7.0. The accumulation of more Na⁺ ions in the forming gel provides increased ion exchange of Na⁺ and Cd²⁺ ions, thereby increasing the efficiency and capacity of

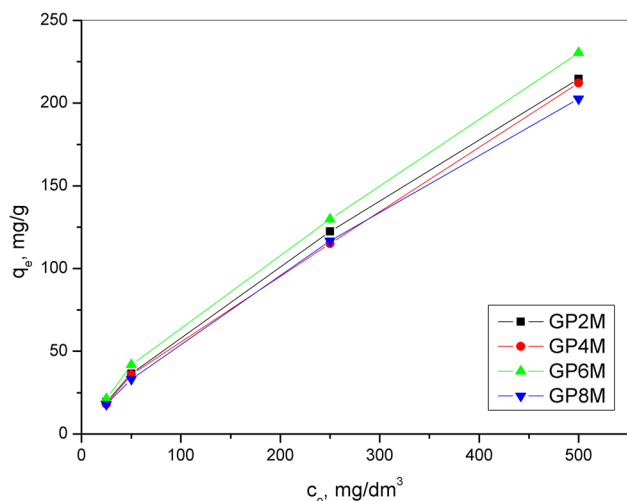


Fig. 8 Effects of initial concentrations cadmium on adsorption capacity of geopolymer ($m_{GP}=0.2500$ g, $t=60$ min, $pH=6.7$)

adsorption. The results obtained in this study are consistent with the findings of other authors [40–42].

3.3.2 Effects of Initial Cadmium Concentration and Dosage of Adsorbents

Figure 8 shows effects of initial cadmium ions concentrations on adsorption capacity onto geopolymer samples. All four samples show a similar dependency trend, but the adsorption capacity for the GP6M geopolymer is somewhat higher.

An increase in the initial concentration of metal leads to an increase in drive force for the adsorption process. This leads to an increase in the adsorption capacity and the adsorption efficiency is high. With a further increase in concentration (from 25.0 to 500.0 mg/dm³), since the amount of adsorbent is constant, due to saturation of the active sites on the geopolymer the adsorption efficiency decreases from 90 to 45%.

The effect of geopolymer dose on the adsorption capacity of Cd(II) ions was investigated in range 0.25–10.0 g/dm³ and the results are shown in Fig. 9. With the increase in geopolymer dose adsorption capacity decreased and became very low for adsorbent dose of 10.0 g/dm³. On contrary, adsorption efficiency increased from 35 to 94% when the adsorbent dose was increased from 0.25 to 10.0 g/dm³. This result could be expected as the active surface of the adsorbent increases as well as the number of active sites that are available for binding of cadmium ions from the solution. It was observed that after geopolymer dose of 2.5 g/dm³ in both cases the plateau was reached and further increment of dose did not have any effect on adsorption capacity and efficiency. The optimum dose of geopolymer to achieve the

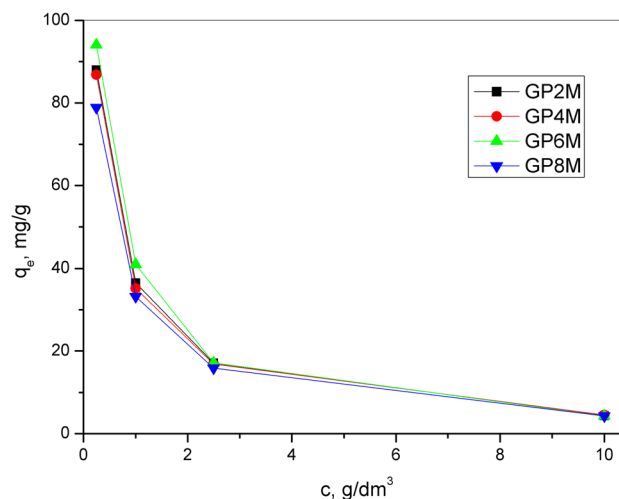


Fig. 9 Effects of adsorbent mass on adsorption capacity of geopolymer samples ($c_0=50$ mg/dm³, $t=60$ min, $pH=6.7$)

high removal efficiency and high capacity for Cd(II) was determined as 1.0 g/dm³. Kara et al. [43] report the similar behavior of metakaolin based geopolymer for adsorption of Zn(II) and Ni(II) ions from aqueous solutions [43]. Comparing the obtained results to literature available results related to adsorption of Cd ions from aqueous solutions using various adsorbents. The adsorption capacity ranges from about 1.0 to 90 mg/g [44–47] depending on the initial concentrations of aqua solutions.

3.3.3 Adsorption Isotherms and Kinetics of Cadmium Ion onto Geopolymer

Adsorption isotherms are used to describe the relationship between adsorbate and adsorbent and to help understand the adsorption mechanism. The distribution of metal ions between solutions and natural adsorbents is most often described using the Langmuir, Freundlich, and Temkin models or Dubinin–Radushkevich [48–50].

Adsorption of cadmium ions on geopolymers can be described with linearized adsorption isotherm in order to determine according to which theoretical model the adsorption process takes place. The experimentally obtained results are fitted to the Langmuir and Freundlich adsorption isotherm. The best agreement with the corresponding model is determined based on the correlation coefficients, R^2 , obtained after the linear fit. For each of the above models, a graph was constructed, which was then linearly fitted. From the slope and intercept q_m , K_L , n , K_F and R^2 were calculated. Based on the obtained correlation coefficients (Table 2), it can be concluded that the experimental results can be well described with both theoretical adsorption models used (R^2

Table 2 Adsorption isotherm model parameters

Models	Parameters	Adsorbents			
		GP2M	GP4M	GP6M	GP8M
Langmuir	q_m	251.89	271.00	256.41	279.33
	K_L	13.52×10^{-3}	11.44×10^{-3}	17.82×10^{-3}	9.36×10^{-3}
	R^2	0.878	0.826	0.930	0.898
Freundlich	N	1.86	1.66	1.97	1.62
	K_F	9.80	7.33	12.62	6.50
	R^2	0.997	0.986	0.992	0.991

≥ 0.90). However, Freundlich's isothermal model yields the best agreement ($R^2=0.99$).

The results obtained in the testing of cadmium ion adsorption kinetics on four geopolymers were fitted with two most commonly used theoretical linearized kinetic models: the kinetics model of the pseudo-first and pseudo-second order [40, 42, 51]. For each of the geopolymer, a graph was constructed, which was then linearly fitted. From the slope and intercept q_e , k_1 , k_2 and R^2 were calculated (Table 3). By comparing correlation coefficients, R^2 , it can be seen that the best matching of experimental results is achieved in the case of the pseudo-second order kinetics model. The pseudo-second order model is based on the assumption that the adsorbent binding of the adsorbent surface is achieved by chemisorption.

Kinetics and adsorption isotherms well explained the adsorption mechanisms for experiments with four geopolymers.

The mechanism of adsorption of heavy metals on geopolymers are still not well understood. In recent years, a lot of studies have been done that have tried to clarify this topic.

Physisorption and chemisorption are two types of adsorption based on the nature of bonds (physical forces and chemical bonds). The adsorbate is attached to the adsorbent surface through Van der Waals forces, electrostatic attraction, ion exchange, ion pairing, hydrophobic or hydrogen bonding. Experimental results indicated that the adsorption process of Cd(II) ions onto different geopolymers includes different adsorption mechanisms. The negative zeta potentials of all geopolymers showed that the electrostatic interactions can play an important role in the cadmium adsorption. Also,

complexation between metal ions and functional groups of adsorbent may be another mechanism responsible for metal removal. Data for all adsorbents fit in Freundlich isotherm better than the Langmuir isotherms. The Freundlich model assumes that the surface of adsorbent is heterogeneous which was confirmed by SEM characterization of investigated adsorbents. During polymerization of aluminosilicate monomers new cation exchange sites were created. By increasing alkalinity, contents of Al and Si decreased to the account of increase in Na content. Sodium ions were available for ion exchange with cadmium ions. Adsorption kinetics is very important for understanding of the determining step of adsorption. Cadmium ions adsorption started rapidly initially. The pseudo-second order equation fitted well for all experiments, which confirmed the chemisorption of metal ions onto geopolymer. Consequently, more than one mechanism was responsible for Cd(II) adsorption process by metakaolin based geopolymer.

Our research are in good agreement with other authors findings regarding the adsorption isotherms Freundlich [42, 47] and Langmuir [45, 46, 52, 53], where kinetics corresponds mainly to the pseudo-second order model.

4 Conclusion

For the purpose of potential use for adsorption of Cd ions from aquas solutions metakaolin based geopolymers were synthesized. The use of different molarity of NaOH as an activator did not lead to large structural differences in the obtained materials. The surface of geopolymer is negatively

Table 3 Kinetics model parameters

Models	Parameters	Adsorbents			
		GP2M	GP4M	GP6M	GP8M
Pseudo-first order	k_1 , 1/min	-1.26×10^{-3}	-2.39×10^{-3}	-1.97×10^{-3}	-3.01×10^{-3}
	q_e , mg/g	0.75	0.64	0.69	0.56
	R^2	0.759	0.854	0.638	0.813
Pseudo-second order	K_2 , g/mg min	15.95×10^{-3}	6.00×10^{-3}	10.63×10^{-3}	5.32×10^{-3}
	q_e , mg/g	37.31	38.87	41.70	37.17
	R^2	0.999	0.998	0.999	0.998

charged and the compound is a condition for the adsorption of the cationic dye existing in aqueous solution.

The better agreement of experimental data with Freundlich isotherm model confirms that adsorption does not take place in the monolayer and that the surface of the geopolymer is heterogeneous. It was found the adsorption capacity increased with an increasing of contact time, pH, and initial concentration in solution and decreased with geopolymer dosage. Namely, the pH value of the solution affects the total charge of the active geopolymer surface. In the acidic environment, the surface is strongly protonated and therefore positively charged. In the base environment, protons are removed from the surface, thereby becoming negatively charged. As the result, attraction of positively charged cadmium ions with the surface of investigated adsorbents is favored in the base environment. Although, some properties of geopolymer labeled as GP6M are different in relation to the other samples. The maximum adsorption efficiency of cadmium ions (84.1%) was achieved at pH > 6 under experimental conditions (room temperature, contact time: 60 min, dose: 1 g/dm³) on adsorbent GP6M. Metakaolin-based geopolymers prepared and investigated in this paper proved to be effective in the process of removing cadmium ions from water.

Acknowledgements This project was financially supported by the Serbian Ministry of Education, Science and Technological Development on projects III 45012 and 172007 and Center for the synthesis, processing and characterization of materials for use in extreme conditions “CEXTREME LAB”.

References

- P.B. Tchounwou, C.G. Yedjon, A.K. Patlolla, D.J. Sutton, *Mol. Clin. Environ. Toxicol.* (2012). https://doi.org/10.1007/978-3-7643-8340-4_6
- S. Sripiboon, K. Suwannahong, T. Kreetachat, N. Kreetachat, *Adv. Environ. Biol.* (2016). <https://doi.org/10.5277/epe150402>
- T. Mathialagan, T. Viraraghavan, *J. Hazard. Mater.* (2002). [https://doi.org/10.1016/S0304-3894\(02\)00084-5](https://doi.org/10.1016/S0304-3894(02)00084-5)
- T.H. Vu, N. Gowripalan, *J. Adv. Concr. Technol.* (2018). <https://doi.org/10.3151/jact.16.124>
- C. Fernández-Pereira, Y. Luna-Galiano, M. Pérez-Clemente, C. Leiva, F. Arroyo, R. Villegas, L.F. Vilches, *Mater. Lett.* (2018). <https://doi.org/10.1016/j.matlet.2018.05.027>
- P. Duxson, J.L. Provis, G. Luckey, J.S.J. van Deventer, *Cem. Concr. Res.* (2007). <https://doi.org/10.1016/j.matlet.2018.05.027>
- G. Habert, J.B. d’Espinoze de Lacaille, N. Roussel, *J. Clean. Prod.* (2011). <https://doi.org/10.1016/j.jclepro.2011.03.012>
- K.A. Komnitsas, *Procedia Eng.* (2011). <https://doi.org/10.1016/j.proeng.2011.11.2108>
- J.L. Provis, S.A. Bernal, *Annu. Rev. Mater. Res.* (2014). <https://www.annualreviews.org/doi/10.1146/annurev-matsci-070813-113515>
- P. De Silva, K. Sago-Crenstil, V. Sirivivatnanon, *Cem. Concr. Res.* (2007). <https://doi.org/10.1016/j.cemconres.2007.01.003>
- J.G.S. Jaarsveld, J.S.J. Deventer, G.C. Lukey, *Chem. Eng. J.* (2002). [https://doi.org/10.1016/S1385-8947\(02\)00025-6](https://doi.org/10.1016/S1385-8947(02)00025-6)
- S. Alonso, A. Palomo, *Cem. Concr. Res.* (2001). [https://doi.org/10.1016/S0008-8846\(00\)00435-X](https://doi.org/10.1016/S0008-8846(00)00435-X)
- M.L. Granizo, S. Alonso, M.T. Blanco-Varela, A. Palomo, *J. Am. Ceram. Soc.* (2002). <https://doi.org/10.1111/j.1151-2916.2002.tb00070.x>
- S.V. Patankar, Y.M. Ghugal, S.S. Jamkar, *Indian J. Mater. Sci.* (2014). <https://doi.org/10.1155/2014/938789>
- K. Parthiban, K.S.R. Mohan, *Int. J. Chem. Tech Res.* **6**, 2446–2450 (2014)
- A.B. Malkawia, M.F. Nuruddina, A. Fauzia, H. Almat-tarneh, B.S. Mohammed, *Procedia Eng.* (2016). <https://doi.org/10.1016/j.proeng.2016.06.581>
- C.N. Livi, W.L. Repette, *IBRACON Struct. Mater. J.* (2017). <https://doi.org/10.1590/s1983-41952017000600003>
- A. Nmiri, N. Hamdi, O. Yazoghli-Marzouk, M. Duc, E. Srasra, *J. Mater. Environ. Sci.* **8**, 676–690 (2017). https://www.jmaterenvironsci.com/Document/vol8/vol8_N2/73-JMES-2404-Nmiri.pdf
- S.V. Patankar, S.S. Jamkar, D.D. More, *Int. J. Eng. Technol. Manage. Appl. Sci.* **5**(1), 114–122 (2017)
- S. Nenadović, L.J. Kljajević, M. Nenadović, M. Mirković, S. Marković, Z. Rakočević, *Environ. Earth Sci.* (2015). <https://doi.org/10.1007/c12665-014-3941-y>
- A. Palomo, F. Glasser, *Br. Ceram. Trans. J.* **91**, 107–112 (1992)
- J.L. Provis, G.C. Lukey, J.S. van Deventer, *Chem. Mater.* (2005). <https://doi.org/10.1021/cm050230i>
- N. Lee, H.R. Khalid, H. Lee, *Microporous Mesoporous Mater.* (2016). <https://doi.org/10.1016/j.micromeso.2016.04.016>
- L.J. Janik, J.O. Skjemstad, *Aust. J. Soil Res.* (1995). <https://doi.org/10.1071/SR9950637>
- T. Armaroli, T. Bécue, S. Gautier, *Oil Gas Sci. Technol. Rev. IFP* (2004). <https://doi.org/10.2516/ogst.2004016>
- G. Accardo, R. Cioffi, F. Colangelo, R. d’Angelo, L. De Stefano, F. Paglietti, *Materials* (2014). <https://doi.org/10.3390/ma7010457>
- J.G.S. Van Jaarsveld, J.S.J. van Deventer, G.C. Lukey, *Mater. Lett.* **57**, 1272–1280 (2003)
- V.F.F. Barbosa, K.J.D. MacKenzie, C. Thaumaturgo, *Int. J. Inorg. Mater.* **2**, 309–317 (2000)
- M. Kapur, M.K. Mondal, *J. Taiwan Inst. Chem. Eng.* **45**, 1803–1813 (2014)
- Y. Zhang, W. Sun, Z. Li, *J. Wuhan Univ. Technol.* **23**, 522–527 (2008)
- L.M. Kljajević, S.S. Nenadović, M.T. Nenadović, N.K. Bundaleski, B.Ž. Todorović, V.B. Pavlović, Z.L. Rakočević, *Ceram. Int.* **43**, 6700–6708 (2017)
- C. Karlsson, E. Zanghellini, J. Swenson, B. Roling, D.T. Bowron, L. Borjesson, *Phys. Rev. B* **72**, 064206 (2005)
- J.L. Provis, C.A. Rees, *Geopolymer synthesis kinetics*, in *Geopolymers: structures, processing, properties and industrial applications*, ed. by J.L. Provis, J.S.J. van Deventer (Woodhead Publishing, Abingdon UK, 2009), pp. 118–136
- P. Innocenzi, *J. Non Cryst. Solids* **316**, 309–319 (2003)
- F. Fondeur, B.S. Mitchell, *Spectrochim. Acta A* (2000). <https://doi.org/10.3390/ma7010457>
- A. Aronne, S. Esposito, C. Ferone, M. Pansini, P. Pernice, *J. Mater. Chem.* **12**, 3039–3045 (2002)
- G. Roviello, L. Ricciotti, C. Ferone, F. Colangelo, R. Cioffi, O. Tarallo, *Materials* **6**, 3943–3962 (2013)
- C. Karlsson, E. Zanghellini, J. Swenson, B. Roling, D.T. Bowron, L. Borjesson, *Phys. Rev. B* **5**, 4 (2005). <https://doi.org/10.1103/PhysRevB.72.064206>
- O.A. Oyetade, V.O. Nyamori, S.B. Jonnalagadda, B.S. Martincigh, *Desalin. Water Treat.* (2018). <https://doi.org/10.5004/dwt.2018.22493>
- Y.-L. Chen, Y.-Y. Tong, R.-W. Pan, J. Tang, *Adv. Mater. Res.* (2013). <https://doi.org/10.4028/www.scientific.net/AMR.704.313>

41. S. Lukman, M.H. Essa, N.D. Mu`azu, A. Bukhari, C. Basheer, J. Environ. Sci. Technol. (2013). <https://scialert.net/abstract/?doi=jest.2013.1.15>
42. H. Javadian, F. Ghorbani, H.-A. Tayebi, S.M.H. Asl, Arab. J. Chem. (2015). <https://doi.org/10.1016/j.arabjc.2013.02.018>
43. I. Kara, D. Yilmazer, S.T. Akar, Appl. Clay Sci. (2017). <https://doi.org/10.1016/j.clay.2017.01.008>
44. Y.F. Jia, K.M. Thomas, Langmuir **16**(3), 1114–1122 (2000)
45. E. Cheraghi, E. Ameri, A. Moheb, Int. J. Environ. Sci. Technol. **12**, 2579–2592 (2015)
46. A. Kakaei, M. Kazemeini, Iran. J. Toxicol. **10**(1), 9–14 (2016)
47. M. Tanzifi, M.K. Nezhad, K. Karimipour, J. Water Environ. Nanotechnol. **2**(4), 265–277 (2017)
48. A.O. Dada, A.P. Olalekan, A.M. Olatunya, O. Dada, IOSR J. Appl. Chem. (2012). <https://doi.org/10.9790/5736-0313845>
49. S.A. Sadeek, N.A. Negm, H.H. Hefni, M.M.A. Wahab, Int. J. Biol. Macromol. (2015). <https://doi.org/10.1016/j.ijbiomac.2015.08.031>
50. O. Długosz, M. Banach, J. Mol. Liq. (2018). <https://doi.org/10.1016/j.molliq.2018.03.041>
51. N. Ariffin, M.M. Al Bakri Abdullah, M. R. Rozainy, M.A. Zainol, M.F. Murshed, H. Zain, M.A. Faris, and R. Bayuaji, *MATEC Web of Conferences* 97, 01023, (2017). <https://doi.org/10.1051/mateconf/20179701023>
52. K. Nakamoto, T. Kobayashi, Sep. Sci. Technol. (2018). <https://doi.org/10.1080/01496395.2018.1505914>
53. K.L. Wasewar, P. Kumar, S. Chand, B.N. Padmini, T.T. Teng, Clean: Soil, Air, Water **38**(7), 649–656 (2010)

Publisher's Note Springer Nature remains neutral with regard to jurisdictional claims in published maps and institutional affiliations.